

This is an Open Access document downloaded from ORCA, Cardiff University's institutional repository: <https://orca.cardiff.ac.uk/id/eprint/113137/>

This is the author's version of a work that was submitted to / accepted for publication.

Citation for final published version:

Hao, Cai-Hong, Guo, Xiao-Ning, Meenakshisundaram, Sankar , Yang, Hong, Ma, Ben, Zhang, Yue-Fei, Tong, Xi-Li, Jin, Guo-Qiang and Guo, Xiang-Yun 2018. Synergistic effect of segregated Pd and Au nanoparticles on semiconducting SiC for efficient photocatalytic hydrogenation of nitroarenes. *ACS Applied Materials and Interfaces* 10 (27) , pp. 23029-23036. 10.1021/acsami.8b04044

Publishers page: <http://dx.doi.org/10.1021/acsami.8b04044>

Please note:

Changes made as a result of publishing processes such as copy-editing, formatting and page numbers may not be reflected in this version. For the definitive version of this publication, please refer to the published source. You are advised to consult the publisher's version if you wish to cite this paper.

This version is being made available in accordance with publisher policies. See <http://orca.cf.ac.uk/policies.html> for usage policies. Copyright and moral rights for publications made available in ORCA are retained by the copyright holders.



Synergistic Effect of Segregated Pd and Au Nanoparticles on Semiconducting SiC for Efficient Photocatalytic Hydrogenation of Nitroarenes

Cai-Hong Hao,^{1,5} Xiao-Ning Guo,^{1} Meenakshisundaram Sankar,^{2*} Hong Yang,³ Ben Ma,^{1,5} Yue-Fei Zhang,⁴ Xi-Li Tong,¹ Guo-Qiang Jin,¹ and Xiang-Yun Guo^{1*}*

¹ State Key Laboratory of Coal Conversion, Institute of Coal Chemistry, Chinese Academy of Sciences, Taiyuan, Shanxi 030001, China

² Cardiff Catalysis Institute, School of Chemistry, Cardiff University, Main Building, Park Place, Cardiff CF10 3AT, UK

³ Department of Chemical & Biomolecular Engineering, University of Illinois at Urbana-Champaign, 206 Roger Adams Laboratory, MC-712, 600 South Mathews Avenue, Urbana, Illinois 61801, United States

⁴ Beijing University of Technology, Institute of Microstructure & Property of Advanced Materials, Beijing 100124, China

⁵ University of the Chinese Academy of Sciences, Beijing 100039, China

KEYWORDS: Photocatalytic hydrogenation, synergistic effect, Pd-Au nanoparticles, hydrogen spillover, silicon carbide

ABSTRACT: Efficient catalytic hydrogenation of nitroarenes to anilines with molecular hydrogen at room temperature is still a challenge. In this study, this transformation was achieved by using a photocatalyst of SiC-supported segregated Pd and Au nanoparticles. Under visible light irradiation, the nitrobenzene hydrogenation reached a turnover frequency as high as 1715 h⁻¹ at 25 °C and 0.1 MPa of H₂ pressure. This exceptional catalytic activity is attributed to a synergistic effect of Pd and Au nanoparticles on the semiconducting SiC, which is different from the known electronic or ensemble effects in Pd-Au catalysts. This kind of synergism originates from the plasmonic electron injection of Au and the Mott-Schottky contact at the interface between Pd and SiC. This three-component system changes the electronic structures of SiC surface and produces more active sites to accommodate the atomic hydrogen that spills over from the surface of Pd. These active hydrogen species have weaker interactions with the SiC surface and thus are more mobile than on an inert support, resulting in an ease in reacting with the N=O bonds in nitrobenzene absorbed on SiC to produce aniline.

INTRODUCTION

Anilines are important chemicals and intermediates widely used for the synthesis of dyes, agrochemicals and other fine chemicals.¹⁻³ Industrially, anilines are mainly produced by the catalytic hydrogenation of nitroarenes at high temperatures and pressures, and the global output of anilines has reached more than 4 million tons per annum.⁴ Therefore, any improvements to this hydrogenation process will have a huge economic and environmental impact. Non-noble metal catalysts such as Co₃O₄,⁴ Fe₂O₃,⁵ PV-carbon⁶, noble metal catalysts, such as Au,^{7,8} and bimetallic catalysts, such as AuPt⁹ and CoPd¹⁰ have been investigated to improve the hydrogenation process. Photocatalytic transformation of nitroarenes to anilines is particularly

attractive because it can greatly reduce the energy consumption. However, in most of the photocatalytic hydrogenation routes, hydrogen donors such as formic acid, isopropyl alcohol or triethanolamine were used instead of gaseous H₂.¹¹⁻¹³ Recently, we reported a photocatalytic reduction of nitroarenes with H₂ using graphene-supported CoS₂ particles as the catalyst under mild condition, however with unsatisfactory activity.¹⁴

For catalytic hydrogenation of nitroarenes, dissociation of H₂ is the rate-determining step.^{9,15,16} Corma et al. reported that the hydrogenation of nitrostyrene over Au/TiO₂ catalyst proceeds via a cooperative effect in which Au sites dissociate H₂ and TiO₂ adsorbs nitrostyrene.¹⁷ However, similar cooperative effect was not observed for other supports such as SiO₂ or carbon. This unique effect for TiO₂ supported catalyst is attributed to the semiconducting properties of TiO₂. Cubic SiC is a semiconductor with a band gap of ca. 2.4 eV, which can absorb visible light. Previous studies have shown that Pd/SiC and Au/SiC catalysts exhibit good photocatalytic activity for the hydrogenation of furan and cinnamaldehyde.^{18,19} These excellent photocatalytic performances of SiC-based catalysts are attributed to the absorption of visible light by SiC and the charge transfer between metals and SiC. Inspired by these results, we hypothesize that bimetallic Pd-Au nanoparticles supported on SiC may show unusual performances for the hydrogenation of nitroarenes.

Pd-Au bimetallic catalysts exhibit markedly enhanced catalytic activity for selective oxidation, selective hydrogenation and other organic transformations,²⁰⁻²⁵ which is mainly caused by a synergism between Au and Pd including electronic and ensemble effect.²⁶ In the electronic effect, electron transfer occurs between Au and Pd, resulting in charge-heterogeneous active sites.^{21,26} In the ensemble effect, the role of Au is to isolate or dilute single Pd sites or ensembles.²⁷ Depending on catalytic reactions and reaction conditions, either one or both of these effects are

involved. In almost all reports, the two metals are in close contact either in core-shelled or alloyed nanostructures.^{28,29} In this work, we report that segregated Pd and Au nanoparticles supported on SiC display a novel synergistic effect that changes the electronic structure of support surface, and thus exhibit significantly enhanced photocatalytic activity for the nitroarene hydrogenation.

EXPERIMENTAL METHODS

Preparation of catalysts. The SiC-supported 3 wt% Pd and 0.5 wt% Au catalyst ($\text{Pd}_3\text{Au}_{0.5}/\text{SiC}$) was prepared via the reduction of $\text{Pd}(\text{NO}_3)_2$ and HAuCl_4 in succession. Firstly, 965 mg of SiC powders were dispersed into 28.2 mL of $\text{Pd}(\text{NO}_3)_2$ aqueous solution (0.01 M). 20 mL of lysine aqueous solution (0.53 M) was dropwise added into the above suspension under stirring for 30 min. 10 mL of NaBH_4 solution (0.35 M) was added in 20 min, and then 10 mL of 0.3 M HCl was dropwise added to the above suspension. The mixture was placed under stirring for 24 h. Next, 4.3 mL of HAuCl_4 aqueous solution (2 mg/mL) was added and stirred for 2 h. Finally, the mixture was separated, washed and dried to obtain $\text{Pd}_3\text{Au}_{0.5}/\text{SiC}$ catalyst. Other catalysts were prepared by the similar way.

Characterizations. The high-resolution transmission electron microscopy (HRTEM, JEM-2100F) and high-angle annular dark field scanning transmission electron microscopy (HAADF-STEM) were used to investigate the microstructures of catalysts. X-ray photoelectron spectroscopy (XPS) was measured using Al Ka ($h\nu=1486.6$ eV) X-ray line on a Kratos XSAM800 spectrometer. X-ray diffractometer (XRD, Rigaku D-Max/RB) were used to characterize the crystalline phases. Diffusive reflectance UV-visible absorption spectra were measured with Al_2O_3 as the reference using a UV-3600 spectrophotometer (Shimadzu). The

photoluminescence (PL) spectra were recorded on F-7000 spectrofluorometer with an excitation wavelength of 320 nm (with a 390 nm filter) at room temperature.

Pulse hydrogen adsorption and temperature programmed desorption (TPD). 50 mg of catalyst sample was pretreated in Ar flow (25 mL/min) at 400 °C for 2 h, and then cooled to room temperature. After the pretreatment, H₂ was inducted to the sample in the form of pulse injection for 10-20 min until adsorption saturation. After pulse H₂ adsorption, the system was purged with Ar (25 mL/min) until the signal reduced to constant. The temperature was ramped from 25 to 900 °C with a rate of 5 °C/min in Ar (25 mL/min).

In-situ diffuse reflectance FT-IR measurement. Catalyst powders (ca. 20 mg) were placed in an in-situ IR cell with a heatable holder. The cell has multiple gas inlets for introduction of Ar or H₂/Ar and an outlet for exhaust. Gas flow was controlled by mass flow controllers. In-situ diffuse reflectance FT-IR measurements were performed on a TENSOR27 infrared spectrometer with a resolution of 8 cm⁻¹. The sample was firstly heated to 400 °C at 5 °C/min in Ar atmosphere with a flow rate of 60 mL/min, and kept under these conditions for 2 h, then cooled to 25 °C. A spectrum was taken for use as a background. Nitrobenzene was introduced to the catalyst sample, and then the sample cell was purged again using the Ar flow to remove non-adsorbed nitrobenzene until a constant spectral signal was reached. H₂/Ar (5 vol%) flow of 20 mL/min was introduced into the cell, and the IR spectra were recorded.

Test of catalyst activity. The reactant suspension consisted of 6 mmol of nitroarene, 25 mg of Pd₃Au_{0.5}/SiC catalyst and 10 mL of anhydrous ethanol. The reactions were conducted in ambient H₂ flow at 25 °C under Xe-lamp irradiation (400-800 nm) with light intensity of 0.8 W·cm⁻². Dependence of the catalytic activity on the light wavelength was investigated using various low

pass optical filters to block off light below specific cut-off wavelengths while the light intensity remains unchanged. After reaction, qualitative and quantitative analysis of reactants and products were carried out by gas chromatography-mass spectrometry (GC-MS, Bruker SCION SQ 456 GC-MS). The conversion was calculated based on the amount of nitroarene. The turn-over frequency (TOF) was calculated based on the following equation:

$$\text{TOF} = \frac{\text{Amount of nitroarene (mol)} \times \text{conversion (\%)} \times \text{selectivity (\%)}}{\text{Mass of Pd}_3\text{Au}_{0.5}/\text{SiC (g)} \times \text{Pd loading (\%)} \times \text{reaction time (h)}/\text{M}[\text{Pd}] \text{ (g}\cdot\text{mol}^{-1}\text{)}}$$

RESULTS AND DISCUSSION

SiC with a specific surface area of ca. $50 \text{ m}^2\cdot\text{g}^{-1}$ was prepared by a sol-gel and carbothermal reduction method.^{30,31} SiC-supported 3 wt.% Pd and 0.5 wt.% Au catalyst (Pd₃Au_{0.5}/SiC) was prepared via the reduction of Pd(NO₃)₂ and HAuCl₄ in SiC suspension in succession. The photocatalytic performances of different catalysts for the hydrogenation of nitrobenzene with H₂ into aniline were investigated under the irradiation of a 300 W Xe lamp (400-800 nm; $0.8 \text{ W}\cdot\text{cm}^{-2}$). Pure SiC or Au_{0.5}/SiC catalyst did not display any activity for the nitrobenzene hydrogenation with or without irradiation. From Table 1, Pd₃/SiC catalyst gave a photocatalytic nitrobenzene conversion of 42% with a selectivity of 96% for aniline. The photocatalytic activity of the mixture of Pd₃/SiC and Au_{0.5}/SiC was 46% with a selectivity of 97% for aniline. It can be seen that the addition of Au/SiC has a little contribution to the nitrobenzene conversion. However, when 0.5 wt% of Au was incorporated to the Pd₃/SiC catalyst, a substantial increase in the photocatalytic activity was observed. The bimetallic Pd₃Au_{0.5}/SiC catalyst yielded 100% of nitrobenzene conversion with 100% of aniline selectivity. The turnover frequency (TOF) was as

high as 1715 h⁻¹, which is one of the highest values reported so far (Table S1) for this reaction. Under the identical reaction condition, Pd₃Au_{0.5}/TiO₂ and Pd₃Au_{0.5}/Al₂O₃ only gave a TOF of 1274 and 951 h⁻¹, respectively. These results suggest the important role of SiC support in enhancing the intrinsic catalytic activity of the bimetallic Pd-Au nanoparticles. Comparing with those results in dark, the activity and selectivity of four catalysts under irradiation all increased evidently, demonstrating major advantages of the photocatalytic reaction. Particularly, the obvious increments in the selectivity suggest that the photocatalytic hydrogenation obeys an electron-driven route.³²

Table 1. Performances of different catalysts for the hydrogenation of nitrobenzene to aniline under visible light irradiation and in the dark ^a

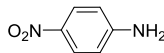
Entry	Catalyst	Conversion (%)		Selectivity (%)		TOF (h ⁻¹)	
		dark	light	dark	light	dark	light
1	Au _{0.5} /SiC	0	0	0	0	0	0
2	Pd ₃ /SiC	11	42	70	96	132±11	691±20
3 ^b	Pd ₃ /SiC+Au _{0.5} /SiC	10	46	75	97	128±17	765±24
4	Pd ₃ Au _{0.5} /SiC	19	100	89	100	290±14	1715±0
5	Pd ₃ Au _{0.5} /TiO ₂	15	75	82	99	211±15	1274±23
6	Pd ₃ Au _{0.5} /Al ₂ O ₃	17	56	78	99	227±21	951±27

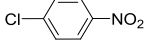
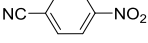
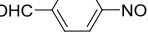
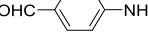
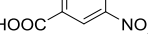
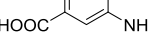
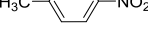
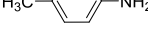
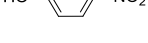
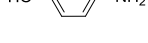
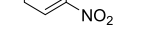
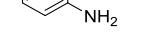
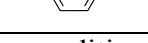
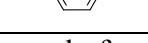
^a The reactions were conducted in flowing atmospheric H₂ at 25 °C using 10 mL anhydrous ethanol mixed with 6 mmol nitrobenzene and 25 mg catalyst. The irradiation intensity was 0.8 W·cm⁻², and the reaction time was 30 min. ^b The catalysts included 25 mg Pd₃/SiC and 25 mg Au_{0.5}/SiC.

The photocatalytic hydrogenation of nitrobenzene over Pd₃Au_{0.5}/SiC using acetonitrile as solvent was also conducted while all the other experimental conditions remained unchanged. The reaction showed a 75% conversion of nitrobenzene with a selectivity of 99% for aniline. When the reaction was conducted using ethanol as solvent but under Ar atmosphere, only 0.5% conversion of nitrobenzene was obtained with 44% of aniline selectivity (the by-products included nitrosobenzene and azobenzene). These results suggest that nitrobenzene reacts with H₂-derived H or alcohol derived H obeys different routes. Therefore, the main H source for nitrobenzene reduction in this work is H₂.

To test the general applicability of this catalyst, a number of substituted nitroarenes were tested under optimized conditions (Table 2). All these nitroarenes were transformed to corresponding anilines over Pd₃Au_{0.5}/SiC catalyst with high activity and selectivity in the presence of irradiation. The nitroarenes with electron-withdrawing groups (entries 1-6) showed higher activity than those with electron-donating groups (entries 7-10), which confirms the nucleophilic reaction mechanism.³³ For p-chloronitrobenzene (entry 3), the low selectivity is due to the dehalogenation reaction.^{12,34} In particular, the nitroarenes with sensitive cyano, aldehyde or carboxyl substituents were also converted selectively into corresponding anilines (entries 4-6). These results demonstrate the general applicability of Pd₃Au_{0.5}/SiC catalyst for the hydrogenation of different nitroarenes with gaseous H₂ to anilines.

Table 2. Photocatalytic hydrogenation of nitroarenes to anilines over Pd₃Au_{0.5}/SiC catalyst ^a

Entry	Reactant	Main product	Time (min)	Conversion (%)	Selectivity (%)	TOF (h ⁻¹)
1			20	100	95	2444±70

2			30	100	80	1372±44
3			25	100	64	1317±61
4			25	100	100	2058±0
5			25	99	98	1997±55
6			25	100	100	2058±0
7			30	100	100	1715±0
8			30	100	100	1715±0
9			30	100	100	1715±0
10			30	100	100	1715±0

^a Reaction conditions: 6 mmol of reactant, 25 mg of Pd₃Au_{0.5}/SiC catalyst in 10 mL of anhydrous ethanol. The reactions were carried out in flowing atmospheric H₂ at 25 °C under Xe-lamp irradiation (400-800 nm) with light intensity of 0.8 W·cm⁻². Products were identified by GC-MS spectrometry.

The recyclability of Pd₃Au_{0.5}/SiC catalyst was investigated by reusing it for five runs under the identical reaction condition. This bimetallic catalyst can be reused with no measureable loss in both the catalytic activity and selectivity, proving its excellent stability and reusability (Figure S1a). TEM images of the catalyst after five runs show no obvious change in the particle size and morphology of both Au and Pd nanoparticles (Figure S1b). The XRD results of the used catalyst also suggest that the Pd and Au nanoparticles still exist on the SiC surface as metallic phase (Figure S1c).

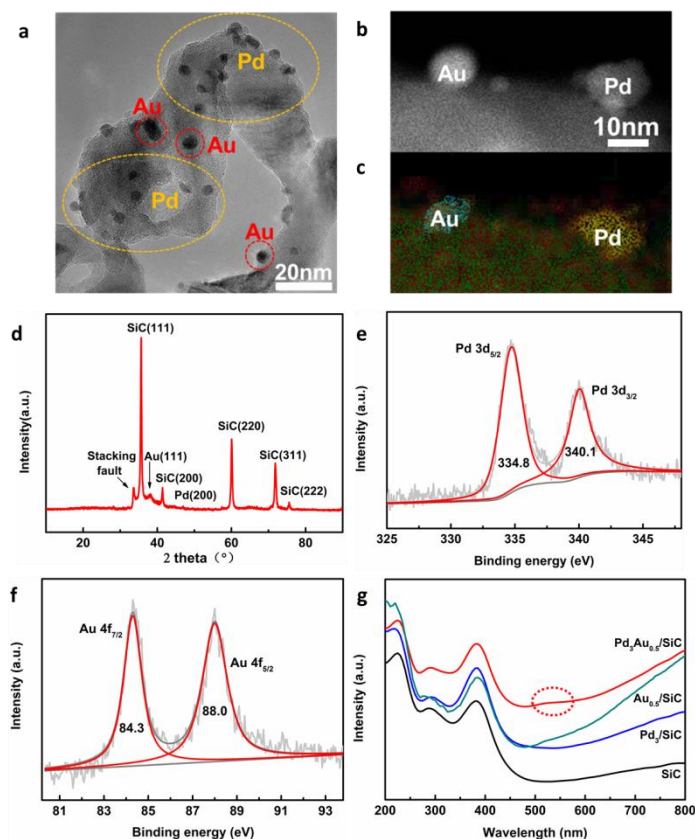


Figure 1. (a) TEM image, (b) HAADF-STEM image of a Pd nanoparticle and Au nanoparticle and, (c) its corresponding high resolution elemental mapping (Au/blue, Pd/yellow, Si/green and C/red), (d) XRD patterns, (e), (f) XPS of Pd₃Au_{0.5}/SiC catalyst. (g) UV-Vis absorption spectra of different catalysts. The circle in (g) indicates the absorption caused by the localized surface plasmon resonance of Au nanoparticles.

Different microscopic and spectroscopic methods were used to characterize the structural features of Pd₃Au_{0.5}/SiC catalyst. The transmission electron microscopic images (TEM) of Pd₃Au_{0.5}/SiC (Figure 1a and S2) show that the metallic nanoparticles are in the size range of 2-14 nm. From the high-angle annular dark field scanning TEM (HAADF-STEM) results (Figure 1b), Pd and Au in the catalyst exist as segregated monometallic nanoparticles with average diameters about 3.9 and 8.2 nm, respectively (Figure S3). This monometallic particle segregation is further

confirmed by the high-resolution elemental mapping of Pd₃Au_{0.5}/SiC (Figure 1c). From the XRD patterns of the catalyst (Figure 1d), the diffraction peaks of face-centered cubic Au and Pd metals are clearly visible and the positions of Pd diffraction peaks do not shift (Figure S4). These results indicate that here, unlike Pd-Au alloys, there is no intimate mixing of Pd and Au nanoparticles. We also prepared SiC supported Pd-Au nanoparticles in alloyed nanostructure with the same loadings by simultaneously reduction of Pd and Au salts in a SiC suspension (Figure S5). The alloyed Pd₃-Au_{0.5}/SiC catalyst just yielded 70% of nitrobenzene conversion with 99% of aniline selectivity. The activity is lower than the present Pd₃Au_{0.5}/SiC catalyst, indicating the two catalysts possess different nanostructures. From the X-ray photoelectron spectroscopy (XPS) results of Pd₃Au_{0.5}/SiC, the binding energy (BE) of Pd 3d_{5/2} shifts slightly from 335.0 eV to lower values of 334.8 eV, relative to Pd/SiC (Figure S6a), suggesting an electron-enrichment on Pd (Figure 1e), while the BE value of Au 4f_{7/2} increases from 84.1 eV to 84.3 eV, relative to Au/SiC (Figure S6b), indicating a further electron-deficiency on Au (Figure 1f). This suggests electron transfer at the Pd/SiC and Au/SiC interfaces, which results from the Mott-Schottky contact and the injection of Au plasmonic electrons, respectively.^{35,36} From the ultraviolet-visible (UV-Vis) spectra (Figure 1g), Au_{0.5}/SiC, Pd₃/SiC and Pd₃Au_{0.5}/SiC show strong absorption in both UV and visible range compared to pure SiC, indicating that these supported nanoparticles can efficiently exploit the light energy. The strong absorption appearing at about 375 nm comes from SiC, while the very weak peak at approximately 520 nm is due to the localized surface plasmon resonance absorption of Au nanoparticles.³⁷ Compared to pure SiC, the photoluminescence (PL) intensities of Au_{0.5}/SiC, Pd₃/SiC and Pd₃Au_{0.5}/SiC show obvious decrease (Figure S7a), indicating that the recombination of photo-generated electrons and holes in SiC has been effectively suppressed. Time-resolved transient PL decay spectra were employed

to investigate the rate of carrier recombination. From the spectra (Figure S7b), pure SiC has the longest PL lifetime ($\tau= 6.17$ ns). However, the lifetime decreases to 5.39, 5.22 and 5.21 ns for Au_{0.5}/SiC, Pd₃/SiC and Pd₃Au_{0.5}/SiC, respectively, indicating that the photo-generated charges have been efficiently separated. The significant contribution of light irradiation to the catalyst activity can be clearly seen from Table 1, and it can be further confirmed by the dependences of catalytic activity on the irradiation intensity and wavelength (Figure S8).

Since the dissociation of H₂ is the rate-determining step for nitrobenzene hydrogenation, catalysts that effectively dissociate H₂ can greatly improve the reaction activity.⁹ To confirm this, the H₂ chemisorption capacity of a series of catalysts was measured by pulse adsorption at room temperature (Figure 2a and Table S2). The saturation adsorption of H₂ on pure SiC support was 630.4 $\mu\text{mol}\cdot\text{g}^{-1}$, while that of Pd₃/SiC was 1357.7 $\mu\text{mol}\cdot\text{g}^{-1}$. By incorporating Au to the Pd catalyst, Pd₃Au_{0.5}/SiC showed an enhanced H₂ capacity of 1803.7 $\mu\text{mol}\cdot\text{g}^{-1}$, suggesting an interesting synergistic effect for H₂ chemisorption. This trend directly correlates with the catalytic activities observed for these catalysts. Based on the chemisorption result of Pd₃/SiC, the atomic ratio of H/Pd is about 9.6. The high H/Pd ratio indicates that most of hydrogen species are adsorbed on SiC surface and the hydrogen on SiC possibly results from the spillover from Pd particles. The saturation adsorption of H₂ on Pd₃Au₁/SiC is close to Pd₃Au_{0.5}/SiC, while it decreases with further increasing the mass ratio of Au/Pd ($> 1/3$). The activities of catalysts with different Au/Pd ratios in 20 min were measured (Figure 2a). It can be found that the activities are in good accordance with the H₂ adsorption capacities. The nitrobenzene conversion (C) increases with the quantity of adsorbed hydrogen atoms (Q_H) based on a power law, $C \propto Q_H^{3.14}$ (Figure S9a). The power law indicates that the hydrogen species adsorbed on SiC surface directly contribute to the reaction.

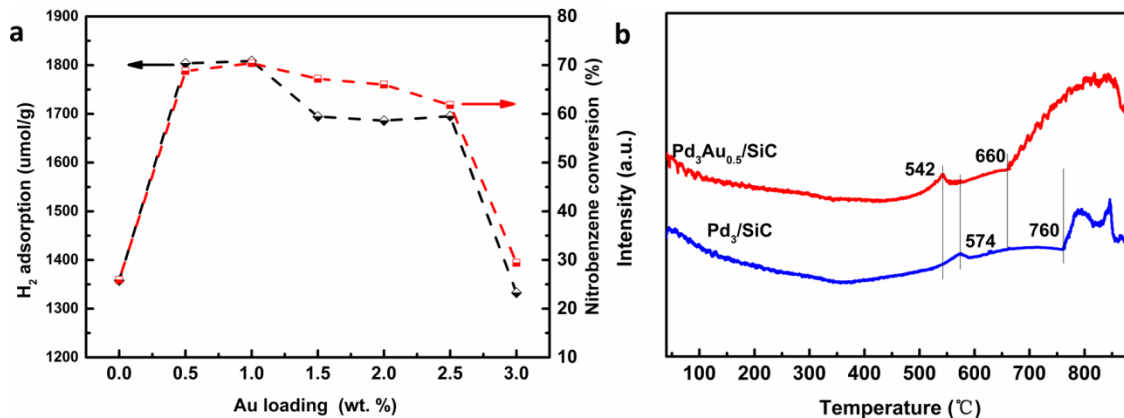


Figure 2. (a) Dependences of H₂ chemisorption capacity and nitrobenzene conversion on different Au loadings in SiC supported Pd-Au catalysts in which the loading level of Pd is constant of 3 wt.%. (b) H₂-TPD profiles of Pd₃/SiC and Pd₃Au_{0.5}/SiC.

H₂-temperature programmed desorption (TPD) is often used to investigate the active sites for H₂ adsorption and to measure the strengths of hydrogen-surface interactions. Yu et al. studied a Pd-Au model catalyst, and reported that hydrogen desorption takes place at ~ -165 °C for monometallic Au, at $\sim 37 - 47$ °C for monometallic Pd, and at ~ -63 °C for the Pd-Au interface sites.³⁸ Ouyang et al. studied Pd-Au/TiO₂ catalysts for synthesis of hydrogen peroxide, and found there were several peaks ranging from 105 to 417 °C in the H₂-TPD spectra, which corresponded to the desorption of H₂ from different Pd sites. The complete desorption of H₂ from Pd-Au/TiO₂ took place before 527 °C.³⁹ Yoo et al. reported that high desorption temperature (> 527 °C) on Pd/Carbon-nanotubes was due to atomic spillover hydrogen that chemisorbed on the dangling bond of carbon surface.⁴⁰ From the H₂-TPD spectra of Pd₃/SiC (Figure 2b), a small H₂ desorption peak appears at about 574 °C, then, huge H₂ desorption starts from 760 °C and continues to above 800 °C. We measured the H₂-TPD spectra of pure SiC and found that H₂ desorption started from 737 °C (Figure S9b). Therefore, the high desorption temperatures in

Figure 2b suggest that H₂ directly desorbs from the SiC surface. Moreover, these results indicate that there exist at least two sites on the SiC surface for H₂ chemisorption, weak and strong chemisorption sites. For Pd₃Au_{0.5}/SiC, the H₂ desorption temperatures from the both sites evidently decreases to 542 and 660 °C, respectively. The decrease of desorption temperatures means that the adsorbed hydrogen species have weaker interactions with SiC surface and thus have higher reactivity. From the TPD results, the addition of Au obviously increases the active sites for H₂ chemisorption but weakens the interactions of atomic hydrogen with SiC surface. The linear sweeping voltammetry curves further confirm this conclusion (Figure S10). The larger oxidation area of Pd₃Au_{0.5}/SiC means more adsorbed hydrogen. The oxidative potential of Pd₃Au_{0.5}/SiC is 0.1 V lower than that of Pd₃/SiC, suggesting that Pd₃Au_{0.5}/SiC has weaker interactions to bond hydrogen atoms. The above results indicate that the addition of Au to Pd₃/SiC has changed the interaction of atomic hydrogen with SiC surface. XPS analysis reveals that the electronic structures of Si 2p and C 1s in SiC have changed. Comparing with pure SiC, the BE values of Si 2p and C 1s in Pd₃Au_{0.5}/SiC decreases from 100.9 eV to 100.6 eV and from 282.9 eV to 282.7 eV, respectively (Figure S11). The decrease of the BE values means that the electrons in SiC can more easily enter atomic orbits of some adsorbates on SiC surface, and thus the ability of SiC surface to bond the adsorbates becomes weak. After treating the catalysts in H₂ at room temperature, the electrical conductivity increased from 6.32×10⁻⁵ to 7.16×10⁻⁵ S·cm⁻¹ for Pd₃/SiC, and from 9.43×10⁻⁵ to 11.0×10⁻⁵ S·cm⁻¹ for Pd₃Au_{0.5}/SiC, respectively. The increase is one of the important characters of hydrogen spillover.⁴¹ Based on Fermi-Dirac statistics, Roland et al. suggested that as an electron donor the spillover hydrogen on the surface of n-type semiconductors could form weak and strong chemisorption species.⁴² Hydrogen donates electrons to the conduction band of n-type SiC resulting in the metallization of SiC surface and

improvement of the electrical conductivity.⁴³ After H₂-treatment, the PL spectra of all catalysts show obvious decrease in the PL intensity (Figure S12), supporting the electron donating.

Although the hydrogen spillover on SiC surface has not been reported yet, numerous studies have revealed that atomic hydrogen can be chemisorbed on SiC surface and the migration of atomic hydrogen on SiC has a very low energy barrier.⁴⁴ Generally, H atoms initially saturate top-layered Si dangling bonds and form strong Si-H with a bond length of about 1.5 Å, and further H atoms then asymmetrically attack weak Si-Si dimers below the top layer and form hydrogen bridge bonds (Si-H-Si) with a Si-H length of 1.68 Å. The electronic nature of SiC surface strongly depends on the hydrogen coverage. Since there are various defect sites on SiC surface, the spillover hydrogen can also be trapped by Si vacancies and form C-H bonds. From the in-situ diffuse reflectance FT-IR spectra of H₂-treated Pd₃Au_{0.5}/SiC (Figure S13), the absorption bands at 2939 and 2057 cm⁻¹ are attributed to the vibration of C-H and Si-H bonds, and the bands at 1502 and 1404 cm⁻¹ are attributed to the hydrogen bridge bonds.^{44,45} However, these absorption bands were not observed in the IR spectroscopy of pure SiC or Au_{0.5}/SiC. From all the above, it is concluded that H₂ can be dissociated on Pd surface and then spillover to various sites of SiC surface. These spillover hydrogen species have lower bonding energies with surface Si atoms and lower barriers for migration on SiC surface, and thus are highly active in chemical reactions.

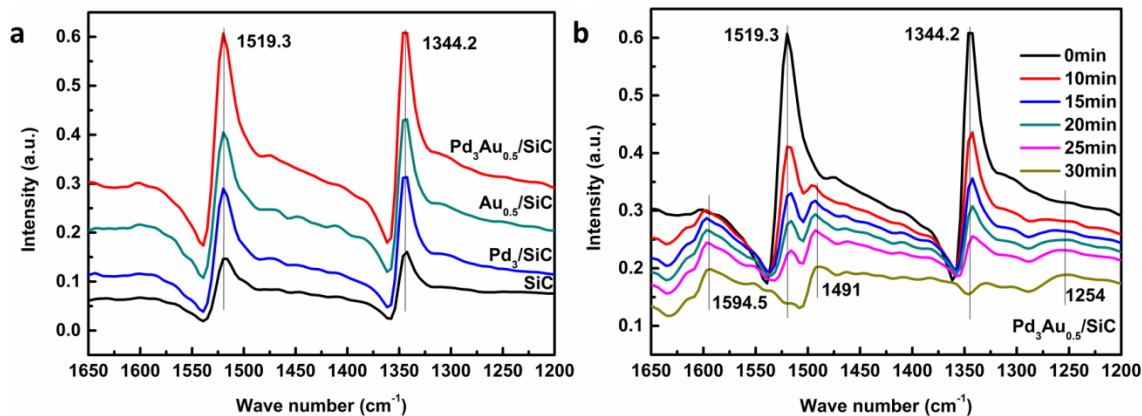


Figure 3. (a) In-situ diffuse reflectance FT-IR spectra of nitrobenzene adsorbed on different catalysts at 25 °C. (b) The evolution of in-situ FT-IR spectra of nitrobenzene adsorbed on Pd₃Au_{0.5}/SiC in a flow of H₂/Ar (5 vol%).

The adsorption of nitrobenzene on SiC surface was also investigated by both experiments and density functional theory (DFT) calculations. From the in-situ diffuse reflectance FT-IR spectra of nitrobenzene adsorbed on the SiC-supported catalysts (Figure 3a), two main absorption bands at 1519.3 and 1344.2 cm⁻¹ are assigned to the asymmetric and symmetric -NO₂ stretching vibrations, respectively.⁴⁶ Compared with those on pure SiC, the absorption bands of -NO₂ show negligible shifts, suggesting that the adsorption of nitrobenzene mainly occurs on the SiC surface rather than Au or Pd surface. With introduction of a H₂/Ar (5 vol%) flow to the nitrobenzene-adsorbed Pd₃Au_{0.5}/SiC, the absorption bands at 1519.3 and 1344.2 cm⁻¹ gradually decrease and finally disappear while the characteristic absorption bands of aniline at 1594.5, 1491 and 1254 cm⁻¹ become more and more evident in 30 min (Figure 3b). The first two belong to the ring stretching vibration in aniline, and the rest one is assigned to the stretching vibration of C-N bond in aniline. The similar FT-IR evolution was not observed on pure SiC or Au_{0.5}/SiC under the identical conditions. Additionally, the absorption bands of -NO₂ on Pd₃Au_{0.5}/SiC can

completely disappear within 2 min by simultaneous introduction of the H₂/Ar flow and the irradiation, suggesting that the important contribution of irradiation on the catalyst activity. These results indicate that the adsorption and hydrogenation of nitrobenzene occurs on the SiC surface.

The density functional theory (DFT) calculations show that nitrobenzene molecules can be adsorbed on SiC(111) surface in both paralleled and vertical modes. However, the paralleled mode yields higher adsorption energy (Table S3), suggesting nitrobenzene molecules tend to adsorb on SiC surface in paralleled mode. Adsorbed nitrobenzene can easily react with atomic hydrogen on SiC(111) surface and produce aniline through direct or condensate route (Figure S14 and S15). Base on the present DFT calculations, aniline is inclined to be produced via the direct route on the hydrogen-rich SiC(111) surface (Table S4). Experimentally, we did not observe other byproducts except nitrosobenzene on SiC-supported catalysts, indicating the reaction is via direct route in this system. We employed pure SiC to catalyze the nitrobenzene hydrogenation at 120 °C. Aniline, azobenzene and azoxybenzene can be detected simultaneously. However, the increase in H₂ pressure is in favor of the production of aniline (Figure S16). This further confirms that the spillover hydrogen on SiC surface largely contributes to the hydrogenation reaction.

The roles of holes in photocatalytic processes are typically complicated.⁴⁷ Under the irradiation, Au nanoparticles generate hot electrons and holes due to the localized surface plasmon resonance. The hot electrons are injected into the conduction band of SiC to activate the –NO₂ group, while the holes on Au nanoparticles are balanced by electrons in the conduction band of SiC. Au has a work function of 5.1 eV, similar to Pd, and SiC has a work function of 4.0 eV. Thus, Schottky contact could form at the interface between Au and SiC due to the difference

in work function between the two. Electrons transfer from SiC to Au in such Schottky contact because SiC is an n-type semiconductor. In this process, SiC provides low-energy electrons to Au and receives hot electrons from Au. Holes on SiC are also very important in this reaction. They result in additional active sites on the SiC surface to accommodate the spillover hydrogen, which acts as an electron donator.⁴²

CONCLUSION

We have shown that isolated Pd and Au nanoparticles on SiC can effectively utilize the visible light to catalyze the hydrogenation of nitrobenzene with molecular hydrogen to form aniline with high activity and selectivity at room temperature. The excellent catalytic performances originate from the good light absorption of the catalyst, the electronic variation of SiC surface due to the synergistic effects from segregated Pd and Au nanoparticles and SiC surface. The Mott-Schottky contact between Pd and SiC can result in electron-rich Pd nanoparticles and heterogeneity in electron distribution on the SiC surface. H₂ dissociates on the electron-rich Pd particles, and then dissociated hydrogen spills over to the SiC surface to form Si-H and C-H bonds. The localized surface plasmon resonance of Au nanoparticles not only results in effective light absorption but also generates energetic electrons on the SiC surface to activate adsorbed nitrobenzene molecules. The atomic hydrogen bonded on the SiC surface thus reacts with the activated nitrobenzene to produce aniline. The Pd₃Au_{0.5}/SiC photocatalyst can be applied to selective hydrogenation of a variety of nitroarenes to corresponding anilines, including many industrially important compounds. The importance of the present work is to reveal a novel synergistic effect of segregated Pd and Au nanoparticles on a semiconducting SiC support. Such configuration and the corresponding catalytic properties of support-mediated synergistic effect can be applied in other complex systems made of metal-semiconducting materials.

ASSOCIATED CONTENT

Supporting Information

Catalyst characterizations, photocatalytic experiments, and computational data are included in Supporting Information. The following files are available free of charge.

Tables S1-S4 and Figures S1-S16 (PDF)

AUTHOR INFORMATION

Corresponding Author

*E-mail: guoxiaoning@sxicc.ac.cn

*E-mail: Sankar@cardiff.ac.uk

*E-mail: xyguo@sxicc.ac.cn

Notes

The authors declare no competing financial interest.

ACKNOWLEDGMENT

X. Y. Guo and M. Sankar thank Prof. G. J. Hutchings for helpful suggestions. The work was financially supported by NSFC (21473232, 21403270, 21673271 and U1710112), SKLCC (2016BWZ005) and YIPA of CAS (2013115).

REFERENCES

(1) He, L.; Wang, L. C.; Sun, H.; Ni, J.; Cao, Y.; He, H. Y.; Fan, K. N. Efficient and Selective Room-Temperature Gold-Catalyzed Reduction of Nitro Compounds with CO and H₂O as the Hydrogen Source. *Angew. Chem. Int. Ed.* **2009**, *48*, 9538-9541.

- (2) Wienhöfer, G.; Sorribes, I.; Boddien, A.; Westerhaus, F.; Junge, K.; Junge, H.; Llusar, R.; Beller, M. General and Selective Iron-Catalyzed Transfer Hydrogenation of Nitroarenes without Base. *J. Am. Chem. Soc.* **2011**, *133*, 12875-12879.
- (3) Chen, P. R.; Khetan, A.; Yang, F. K.; Migunov, V.; Weide, P.; Stürmer, S. P.; Guo, P. H.; Kähler, K.; Xia, W.; Mayer, J.; Pitsch, H.; Simon, U.; Muhler, M. Experimental and Theoretical Understanding of Nitrogen-Doping-Induced Strong Metal-Support Interactions in Pd/TiO₂ Catalysts for Nitrobenzene Hydrogenation. *ACS Catal.* **2017**, *7*, 1197-1206.
- (4) Westerhaus, F. A.; Jagadeesh, R. V.; Wienhöfer, G.; Pohl, M. M.; Radnik, J.; Surkus, A. E.; Rabeah, J.; Junge, K.; Junge, H.; Nielsen, M.; Brückner, A.; Beller, M. Heterogenized Cobalt Oxide Catalysts for Nitroarene Reduction by Pyrolysis of Molecularly Defined Complexes. *Nat. Chem.* **2013**, *5*, 537-543.
- (5) Jagadeesh, R. V.; Surkus, A. E.; Junge, H.; Pohl, M. M.; Radnik, J.; Rabeah, J.; Huan, H. M.; Schünemann, V.; Brückner, A.; Beller, M. Nanoscale Fe₂O₃-Based Catalysts for Selective Hydrogenation of Nitroarenes to Anilines. *Science* **2013**, *342*, 1073-1076.
- (6) Gao R. V.; Pan L.; Lu, J. H.; Xu J. S.; Zhang, X. W.; Wang, L.; Zou J. J. Phosphorus-Doped and Lattice-Defective Carbon as Metal-Like Catalyst for Selective Hydrogenation of Nitroarenes. *ChemCatChem* **2017**, *9*, 4287-7294.
- (7) Corma, A.; Serna, P. Chemoselective Hydrogenation of Nitro Compounds with Supported Gold Catalysts. *Science* **2006**, *313*, 332-334.
- (8) Wang, L.; Zhang, J.; Wang, H.; Shao, Y.; Liu, X. H.; Wang, Y. Q.; Lewis, J. P.; Xiao, F. S. Activity and Selectivity in Nitroarene Hydrogenation over Au Nanoparticles on the Edge/Corner of Anatase. *ACS Catal.* **2016**, *6*, 4110-4116.

- (9) Serna, P.; Concepción, P.; Corma, A. Design of Highly Active and Chemoselective Bimetallic Gold-Platinum Hydrogenation Catalysts through Kinetic and Isotopic Studies. *J. Catal.* **2009**, *265*, 19-25.
- (10) Shen, K.; Chen, L.; Long, J. L.; Zhong, W.; Li, Y. W. MOFs-Templated Co@Pd Core-Shell NPs Embedded in N-Doped Carbon Matrix with Superior Hydrogenation Activities. *ACS Catal.* **2015**, *5*, 5264-5271.
- (11) Tsutsumi, K.; Uchikawa, F.; Sakai, K.; Tabata, K. Photoinduced Reduction of Nitroarenes Using a Transition-Metal-Loaded Silicon Semiconductor under Visible Light Irradiation. *ACS Catal.* **2016**, *6*, 4394-4398.
- (12) Xiao, Q.; Sarina S.; Waclawik, E. R.; Jia, J. F.; Chang, J.; Riches, J. D.; Wu, H. S.; Zheng, Z. F.; Zhu, H. Y. Alloying Gold with Copper Makes for a Highly Selective Visible-Light Photocatalyst for the Reduction of Nitroaromatics to Anilines. *ACS Catal.* **2016**, *6*, 1744-1753.
- (13) Földner, S.; Pohla, P.; Bartling, H.; Dankesreiter, S.; Stadler, R.; Gruber, M.; Pfitzner, A.; König, B. Selective Photocatalytic Reductions of Nitrobenzene Derivatives Using PbBiO₂X and Blue Light. *Green Chem.* **2011**, *13*, 640-643.
- (14) Ma, B.; Wang, Y. Y.; Tong, X. L.; Guo, X. N.; Zheng, Z. F.; Guo, X. Y. Graphene-Supported CoS₂ Particles: An Efficient Photocatalyst for Selective Hydrogenation of Nitroaromatics in Visible Light. *Catal. Sci. Technol.* **2017**, *7*, 2805-2812.
- (15) Ohyama, J.; Esaki, A.; Koketsu, T.; Yamamoto, Y.; Arai, S.; Satsuma, A. Atomic-Scale Insight into the Structural Effect of a Supported Au Catalyst Based on a Size-Distribution Analysis Using Cs-STEM and Morphological Image-Processing. *J. Catal.* **2016**, *335*, 24-35.

- (16) Song J. J.; Huang, Z. F.; Pan, L.; Li, K.; Zhang, X. W.; Wang, L.; Zou, J. J. Review on Selective Hydrogenation of Nitroarene by Catalytic, Photocatalytic and Electrocatalytic Reactions. *Appl. Catal. B-Environ.* **2018**, *227*, 386-408.
- (17) Boronat, M.; Concepción, P.; Corma, A.; González, S.; Illas, F.; Serna, P. A Molecular Mechanism for the Chemoselective Hydrogenation of Substituted Nitroaromatics with Nanoparticles of Gold on TiO₂ Catalysts: A Cooperative Effect between Gold and the Support. *J. Am. Chem. Soc.* **2007**, *129*, 16230-16237.
- (18) Jiao, Z. F.; Guo, X. N.; Zhai, Z. Y.; Jin, G. Q.; Wang, X. M.; Guo, X. Y. The Enhanced Catalytic Performance of Pd/SiC for the Hydrogenation of Furan Derivatives at Ambient Temperature under Visible Light Irradiation. *Catal. Sci. Technol.* **2014**, *4*, 2494-2498.
- (19) Hao, C. H.; Guo, X. N.; Pan, Y. T.; Chen, S.; Jiao, Z. F.; Yang, H.; Guo, X. Y. Visible-Light-Driven Selective Photocatalytic Hydrogenation of Cinnamaldehyde over Au/SiC Catalysts. *J. Am. Chem. Soc.* **2016**, *138*, 9361-9364.
- (20) Lee, Y. W.; Kim, M.; Kim, Z. H.; Han, S. W. One-Step Synthesis of Au@Pd Core-Shell Nanooctahedron. *J. Am. Chem. Soc.* **2009**, *131*, 17036-17037.
- (21) Zhang, H. J.; Watanabe, T.; Okumura, M.; Haruta, M.; Toshima, N. Catalytically Highly Active Top Gold Atom on Palladium Nanocluster. *Nat. Mater.* **2012**, *11*, 49-52.
- (22) Enache, D. I.; Edwards, J. K.; Landon, P.; Solsona-Espriu, B.; Carley, A. F.; Herzing, A. A.; Watanabe, M.; Kiely, C. J.; Knight, D. W.; Hutchings, G. J. Solvent-Free Oxidation of Primary Alcohols to Aldehydes Using Au-Pd/ TiO₂ Catalysts. *Science* **2006**, *311*, 362-365.
- (23) Hutchings, G. J. Nanocrystalline Gold and Gold Palladium Alloy Catalysts for Chemical Synthesis. *Chem. Commun.* **2008**, *10*, 1148-1164.

- (24) Kolli, N. E.; Delannoy, L.; Louis, C. Bimetallic Au-Pd Catalysts for Selective Hydrogenation of Butadiene: Influence of the Preparation Method on Catalytic Properties. *J. Catal.* **2013**, *297*, 79-92.
- (25) Sarina, S.; Zhu, H. Y.; Jaatinen, E.; Xiao, Q.; Liu, H. W.; Jia, J. F.; Chen, C.; Zhao, J. Enhancing Catalytic Performance of Palladium in Gold and Palladium Alloy Nanoparticles for Organic Synthesis Reactions through Visible Light Irradiation at Ambient Temperatures. *J. Am. Chem. Soc.* **2013**, *135*, 5793-5801.
- (26) Wang, A. Q.; Liu, X. Y.; Mou, C. Y.; Zhang, T. Understanding the Synergistic Effects of Gold Bimetallic Catalysts. *J. Catal.* **2013**, *308*, 258-271.
- (27) Chen, M. S.; Kumar, D.; Yi, C. W.; Goodman, D. W. The Promotional Effect of Gold in Catalysis by Palladium-Gold. *Science* **2005**, *310*, 291-293.
- (28) Gao, F.; Goodman, D. W. Pd-Au Bimetallic Catalysts: Understanding Alloy Effects from Planar Models and (Supported) Nanoparticles. *Chem. Soc. Rev.* **2012**, *41*, 8009-8020.
- (29) Jiang, H. L.; Xu, Q. Recent Progress in Synergistic Catalysis over Heterometallic Nanoparticles. *J. Mater. Chem.* **2011**, *21*, 13705-13725.
- (30) Jin, G. Q.; Guo, X. Y. Synthesis and Characterization of Mesoporous Silicon Carbide. *Micropor. Mesopor. Mater.* **2003**, *60*, 207-212.
- (31) Jiao, Z. F.; Zhai, Z. Y.; Guo, X. N.; Guo, X. Y. Visible-Light-Driven Photocatalytic Suzuki-Miyaura Coupling Reaction on Mott-Schottky-type Pd/SiC Catalyst. *J. Phys. Chem. C* **2015**, *119*, 3238-3243.
- (32) Linic, S.; Aslam, U.; Boerigter, C.; Morabito, M. Photochemical Transformations on Plasmonic Metal Nanoparticles. *Nat. Mater.* **2015**, *14*, 567-576.

- (33) Cárdenas-Lizana, F.; Berguerand, C.; Yuranov, I.; Kiwi-Minsker, L. Chemoselective Hydrogenation of Nitroarenes: Boosting Nanoparticle Efficiency by Confinement within Highly Porous Polymeric Framework. *J. Catal.* **2013**, *301*, 103-111.
- (34) Cárdenas-Lizana, F.; Hao, Y. F.; Crespo-Quesada, M.; Yuranov, I.; Wang, X. D.; Keane, M. A.; Kiwi-Minsker, L. Selective Gas Phase Hydrogenation of p-Chloronitrobenzene over Pd Catalysts: Role of the Support. *ACS Catal.* **2013**, *3*, 1386-1396.
- (35) Li, X. H.; Antonietti, M. Metal Nanoparticles at Mesoporous N-Doped Carbons and Carbon Nitrides: Functional Mott-Schottky Heterojunctions for Catalysis. *Chem. Soc. Rev.* **2013**, *42*, 6593-6604.
- (36) Wu, K.; Chen, J.; McBride, J. R.; Lian, T. Efficient Hot-Electron Transfer by a Plasmon-Induced Interfacial Charge-Transfer Transition. *Science* **2015**, *349*, 632-635.
- (37) Wang, C. L.; Astruc, D. Nanogold Plasmonic Photocatalysis for Organic Synthesis and Clean Energy Conversion. *Chem. Soc. Rev.* **2014**, *43*, 7188-7216.
- (38) Yu, W. Y.; Mullen, G. M.; Flaherty, D. W.; Mullins, C. B. Selective Hydrogen Production from Formic Acid Decomposition on Pd-Au Bimetallic Surfaces. *J. Am. Chem. Soc.* **2014**, *136*, 11070-11078.
- (39) Ouyang, L.; Da, G. J.; Tian, P. F.; Chen, T. Y.; Liang, G. D.; Xu, J.; Han, Y. F. Insight into Active Sites of Pd-Au/TiO₂ Catalysts in Hydrogen Peroxide Synthesis Directly from H₂ and O₂. *J. Catal.* **2014**, *311*, 129-136.
- (40) Yoo, E.; Gao, L.; Komatsu, T.; Yagai, N.; Arai, K.; Yamazaki, T.; Matsuishi, K.; Matsumoto, T.; Nakamura, J. Atomic Hydrogen Storage in Carbon Nanotubes Promoted by Metal Catalysts. *J. Phys. Chem. B* **2004**, *108*, 18903-18907.

- (41) Conner, W. C.; Jr.; Falconer, J. L. Spillover in Heterogeneous Catalysis. *Chem. Rev.* **1995**, *95*, 759-788.
- (42) Roland, U.; Braunschweig, T.; Roessner, F. On the Nature of Spilt-over Hydrogen. *J. Mol. Catal. A: Chem.* **1997**, *127*, 61-84.
- (43) Derycke, V.; Soukiassian, P. G.; Amy, F.; Chabal, Y. J.; D'angelo, M. D.; Enriquez, H. B.; Silly, M. G. Nanochemistry at the Atomic Scale Revealed in Hydrogen-Induced Semiconductor Surface Metallization. *Nat. Mater.* **2003**, *2*, 253-258.
- (44) Pollmann, J.; Peng, X. Y.; Wieferink, J.; Krüger, P. Adsorption of Hydrogen and Hydrocarbon Molecules on SiC(001). *Surf. Sci. Rep.* **2014**, *69*, 55-104.
- (45) Aradi, B.; Gali, A.; Deák, P.; Lowther, J. E.; Son, N. T.; Jánzén, E.; Choyke, W. J. Ab Initio Density-Functional Supercell Calculations of Hydrogen Defects in Cubic SiC. *Phys. Rev. B* **2001**, *63*, 245202-245221.
- (46) Hartfelder, U.; Kartusch, C.; Sá, J.; van Bokhoven, J. A. In Situ Infrared Spectroscopy on the Gas Phase Hydrogenation of Nitrobenzene. *Catal. Commun.* **2012**, *27*, 83-87.
- (47) Peng, T. H.; Miao, J. J.; Gao, Z. S.; Zhang, L. J.; Gao, Y.; Fan, C. H.; Li, D. Reactivating Catalytic Surface: Insights into the Role of Hot Holes in Plasmonic Catalysis. *Small* **2018**, *14*, 1703510-1703516.

SYNOPSIS

